CALCULATION AND DESIGN OF UNDERACTUATED 3-FINGER GRIPPER

TÍNH TOÁN VÀ THIẾT KẾ CƠ CẤU KẸP 3 NGÓN HỤT CƠ CẤU CHẤP HÀNH

Le Hoai Nam[1], Tran Cuong Hung[1], Nguyen Ngoc Linh[1,*]

ABSTRACT

This paper presents work on calculation and design of under-actuated 3-finger gripper which is suitable for research in robot manipulation of objects for industrial and service applications. The conceptualization, the design and the prototype of the gripper are presented, along with the kinematic and static analysis of its mechanism. The proposed versatile gripper is based on a simple mechanism, where the two of the three fingers are under-actuated and driven by a differential mechanism. Also, the plan for the sequence and the synchronization of the movements of the fingers is defined according to the grasping task. Grasping performance of the design is evaluated by using simulation software such as Autodesk Inventor and Matlab/Simulink. After that a prototype of the gripper is produced using 3D printing technique and is integrated with electronic actuation system. The prototype has been tested experimentally under several grasping tasks, where its agility is demonstrated.

Keywords: *Under-actuated 3-finger gripper, differential mechanism, 3D printing, robotics.*

TÓM TẮT

Bài báo này trình bày tính toán và thiết kế bộ gắp 3 ngón hụt cơ cấu chấp hành phù hợp cho nghiên cứu thao tác robot cho các ứng dụng nông nghiệp và dịch vụ. Việc lên ý tưởng, thiết kế và nguyên mẫu của bộ kẹp được trình bày, cùng với phân tích động học và tĩnh học của cơ chế của nó. Bộ gắp đa năng được đề xuất dựa trên một cơ chế đơn giản, trong đó hai trong số ba ngón tay được điều khiển và truyền động thông qua cơ chế vi sai. Khả năng chuyển động và cầm nắm của thiết kế được đánh giá bằng cách sử dụng phần mềm mô phỏng như Autodesk Inventor và Matlab/Simulink. Sau đó, một nguyên mẫu của bộ kẹp được chế tạo bằng kỹ thuật in 3D và được tích hợp hệ thống truyền động điện tử. Các thực nghiệm trong một số nhiệm vụ cầm nắm các vật với hình dạng kích thước khác nhau đã được thực hiện đã cho thấy hiệu quả của thiết kế.

Từ khóa: *Kẹp 3 ngón hụt chấp hành, cơ cấu vi sai, in 3D, robot.*

[1]University of Engineering and Technology - VNU
*Email: nlnguyen@vnu.edu.vn

1. INTRODUCTION

Under-actuation is basically expressing the property of a system to have an input vector of a smaller dimension than the output vector. Practically, in robotics, it means having fewer actuators than degrees of freedom (DOF). Applying this concept to robotic grasping arises from a simple fact: it is desirable to be able to grasp objects using a simple control rather than having to command and coordinate several actions. The idea behind under-actuation in grasping is to use an ingenious mechanical system that can adapt to the shape of the object automatically. This mechanical intelligence, embedded in the hand, is based on the principle of differential mechanism. The latter devices automatically distribute one input to several outputs, the ratio between the different outputs being determined by the design parameters and the output states themselves. The same philosophy of intelligent design is commonly found in mechanical linkages where the different link lengths and joint types are determined at the design stage to follow a particular trajectory.
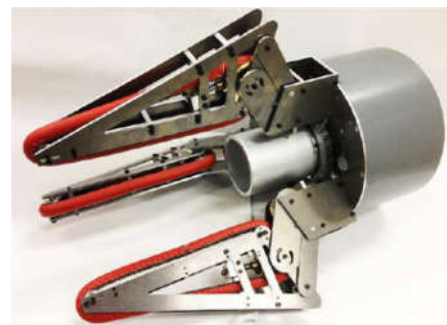
Figure 1. Robotic gripper with three under-actuated finger modules [1]

The development of robotic end effectors that are employed for grasping a variety of objects is an active research area. Some designs use small servomotors in each actuation of each joint of the fingers [11], which ensures a high number of controllable DOFs. This kind of design is suitable for grasping complex shape objects, but it results in high cost and control complexity of the end effector.

Some designs use pulley/tendon actuation mechanisms [5, 6]. These mechanisms have advantages in terms of cost due to a smaller number of actuators, have a high degree of adaptability, and are suitable for different applications but some of their disadvantages include limitations in load-carrying capacity and wear resistance. Some designs use worm gear mechanisms [1, 9]. It has the advantage of a

relatively high payload but because of the worm gears, the grasping is relatively slow.

In this paper, we present a design of an underactuated three-finger gripper. A key characteristic of the presented gripper is the provision of the underactuated within the end effector palm and fingers that provide full enveloping of an object without detailed prior knowledge of its shape. The underactuated between fingers is provided by a combination of differential planetary gear mechanisms and linkage mechanisms, which has novel application to grippers and robotic end effectors. The gripper could prove to be useful for various robotics research and educational projects.

2. MECHANICAL DESIGN

Figure 2. Gripper prototype

2.1. Under-actuated Fingers

The gripper is designed with three fingers to balance the flexibility and complexity of the design. Grippers with a larger number of fingers have the advantages of flexibility in gripping and force distribution, but in return design and control will be complex.

The next parameter to consider is the number of links per finger. The more links a finger has, the more it can conform to an object being grasped, leading to more frictional surface point contacts and less force required to grasp an object. Increasing the number of links leads to added complexity.

According to work done in [8], fingers with 3 links perform 21% better than fingers with 2 links based on a metric of the grasp wrench force required to forcibly remove the object from a stable grasp per unit joint 23 torque. Fingers with a fourth link added only performed 8% better than their 3-linked counterparts Based on the trade-off of grasp efficiency versus mechanical complexity, it was decided this gripper would have 3 links.

Table 1. Fundamental parameters

Design Parameters	Values
Number of Fingers	3
Number of Links per Finger	3
Total Finger Length	120mm
Link 1 Length	65mm
Link 2 Length	35mm
Link 3 Length	20mm
Palm Width	58mm

The finger length must be optimized to meet the requirement of being able to grasp a wide variety of human-sized objects. A total finger length of 120mm was chosen. This size is similar to the prototype grippers that resulted from simulation-based optimization work done by Schuurmans (100mm) [8], Ciocarlie (118mm) [5], and Ma (115mm) [6], among others.
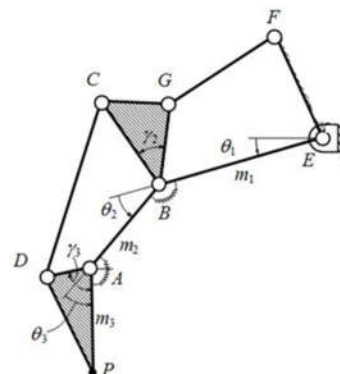
Figure 3. Kinematic sketch of the under-actuated finger mechanism [7]
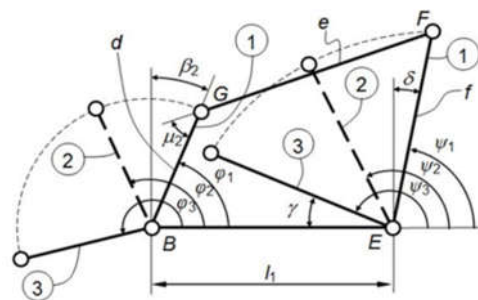
Figure 4. Synthesis of the four bar B, E, F, G [7]
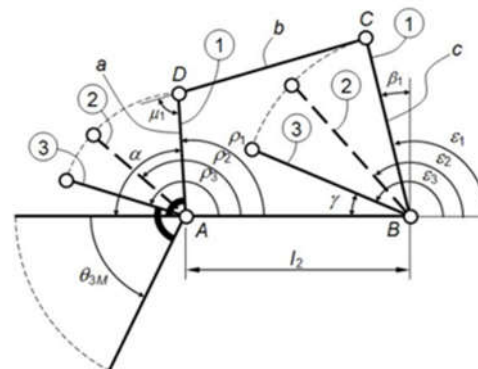
Figure 5. Four bar linkage ABCD [7]

Referring to Fig. 3, the Freudenstein's equations for the four bar linkage ABCD, can be expressed as presented in [4].

$$R_1 \cos \varepsilon_1 - R_2 \cos \rho_1 + R_3 = \cos(\varepsilon_1 - \rho_1)$$
$$R_1 \cos \varepsilon_2 - R_2 \cos \rho_2 + R_3 = \cos(\varepsilon_2 - \rho_2) \quad (1)$$
$$R_1 \cos \varepsilon_3 - R_2 \cos \rho_3 + R_3 = \cos(\varepsilon_3 - \rho_3)$$

$$R_1 = \frac{l_2}{a}; R_2 = \frac{l_2}{c}; R_3 = \frac{a^2 - b^2 + c^2 + l^2}{2ac} \quad (2)$$

The four-bar linkage shown is in equilibrium, let a, b, c and l_2 be the magnitudes of the links AD, DC, BC and AB,

respectively, where l_2 represent the second phalanx. The angles ε_i and ρ_i for i = 1, 2, 3 are the input and output angles of the four-bar linkage of both BC and AD.

Then the pairs of angles (ε_1 = 90°; ρ_1 = 110°), (ε_3 = 116°; ρ_3 = 152,7°) are obtained for the starting and final position respectively of both links AD and BC. As described previously, the initial value of (ε_2 = 100°; ρ_2 = 125°) which correspond to the middle position between the starting and final positions of the links AD and BC, consequently and with β_1 = 30°, α = 15°. Solve the equation (1) and (2) with those three sets of angles, we get our final result a = 17.3mm, b = 46.8mm, c = 25mm.

The same method has been applied to the synthesis of the function generating four-bar linkage B, E, F, G, shown in Fig. 4 the Freudenstein's equation can be expressed in the form:

$$R_1 \cos\psi_1 - R_2 \cos\varphi_1 + R_3 = \cos(\psi_1 - \varphi_1)$$
$$R_1 \cos\psi_2 - R_2 \cos\varphi_2 + R_3 = \cos(\psi_2 - \varphi_2) \qquad (3)$$
$$R_1 \cos\psi_3 - R_2 \cos\varphi_3 + R_3 = \cos(\psi_3 - \varphi_3)$$

$$R_1 = \frac{l_1}{d}; R_2 = \frac{l_1}{f}; R_3 = \frac{d^2 - e^2 + f^2 + l_1^2}{2df} \qquad (4)$$

Where l_1 is the length of the first phalanx, and, d, e and f are the lengths of BG, GF, FE. ψ_i, φ_i for i = 1, 2, 3 are the input and output angels of the links EF and BG, respectively.

Then the pairs of angles (ψ_1 = 105°; φ_1 = 60°), (ψ_3 = 120°; φ_3 = 116°) are obtained for the starting and final position respectively of both links EF and BG. As described previously, the initial value of (ψ_2 = 111°; φ_2 = 90°) which correspond to the middle position between the starting and final positions of the links EF and BG, consequently and with β_2 = 30°, δ = 15°. Solve the equation (3) and (4) with those three sets of angles, we get our final result d = 14.44mm, e = 51.5mm, f = 45mm.

Figure 6. 3D model of the fingers

2.2. Planetary Gear Differential

In the planetary differential, for consistency, the input is chosen to be the carrier torque while the primary and secondary outputs are the sun and annulus torque, as illustrated in Fig. 7.
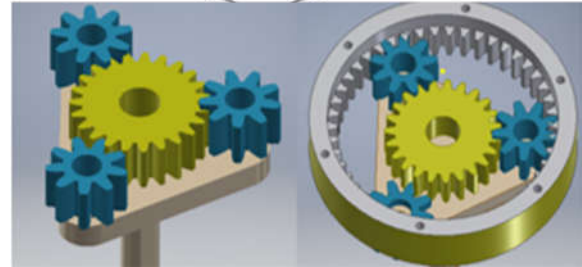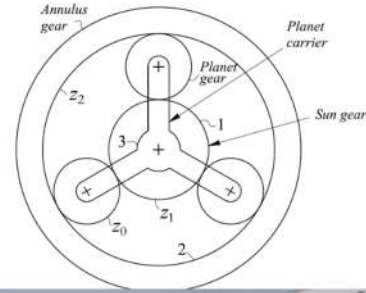
Figure 7. Planetary gear differentials

Therefore, one obtains from [10]:

$$T_3 = T_1 + T_2 \qquad (5)$$

and

$$\frac{T_2}{T_1} = i_0 = \frac{z_2}{z_1} \qquad (6)$$

The planetary differential comprises two planetary gear trains. To obtain a proper distribution of the power, the three output torques should be the same. In the first planetary gear train, the sun gear takes one-third of the input torque and the annulus gear takes two-third of the input torque. The torque in the annulus gear is input for the second planetary gear train. In the second planetary gear train, the sun gear and the annulus gear both take haft of the input torque.

It is noted that force isotropy is impossible to achieve with a simple planetary gear differential because it would require a zero radius of the planet gear. However, to overcome that problem, our second planetary gear train is designed, which the planet consists of two rigidly connected gears instead of a single gear (Fig. 8).
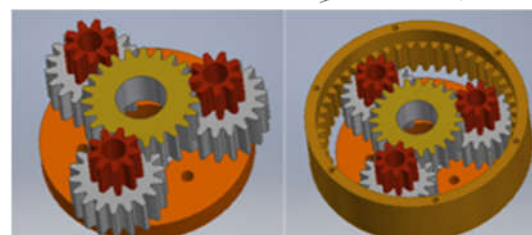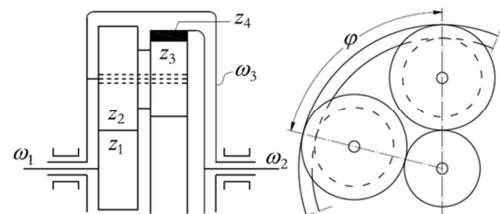
Figure 8. Second planetary gear train

We design the gears by analysis of bending stresses in gear tooth (Fig. 9). First, we analyze the free-body diagram of forces to calculate the torque on each gear and take that result into the bending stress equation to determine the gear parameter. The equation is from [2].
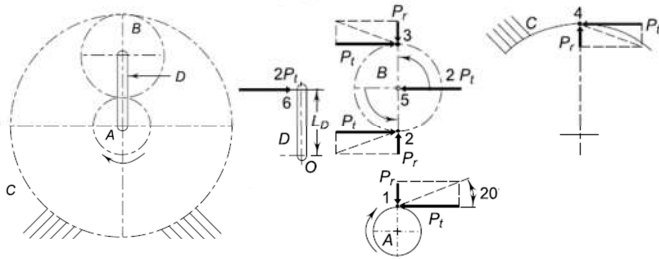
Figure 9. The free-body diagram of forces [2]

$$M_B = P_t \times h; I = \frac{1}{12}bt^3; y = \frac{1}{2}t \tag{7}$$

$$\sigma_b = \frac{M_b y}{I} = \frac{6hP_t}{bt^2} = \frac{S_{ut}}{f_s} = \frac{1}{2}S_{ut} \tag{8}$$

Table 2. First Planetary Gear Train Parameters

Design Parameter	Values
Module	1.5
Centre distance	20mm
Number of teeth of the sun gear	18
Number of teeth of the planet gear	9
Number of teeth of the annulus gear	36
Pitch circle diameters of the sun gear	27mm
Pitch circle diameters of the planet gear	13.5mm
Pitch circle diameters of the annulus gear	54mm
The tooth thickness	10mm

Table 3. Second Planetary Gear Train Parameters

Design Parameter	Values
Module	1.125
Centre distance	18mm
Number of teeth of the sun gear	31
Number of teeth of the first planet gear	21
Number of teeth of the second planet gear	9
Number of teeth of the annulus gear	61
Pitch circle diameters of the sun gear	34.875mm
Pitch circle diameters of the first planet gear	23.625mm
Pitch circle diameters of the second planet gear	10.125mm
Pitch circle diameters of the annulus gear	68.625mm
The tooth thickness	10mm

2.3. Finger Orientation Mechanism

Each of the three identical fingers of gripper is mounted on an additional revolute joint whose axis is located on the vertex of an equilateral triangle and oriented normal to the plane of the triangle. With these additional revolute joints and the orientation mechanism, the hands can be reconfigured by modifying the orientation of the fingers in order to adapt to the general geometry of the object to be grasped.

The main configurations of the fingers are obtained by orienting two of the fingers with a range of 90°, and the rotation of the two fingers is coupled by a gear mechanism shown in Fig. 9. The two sections of gears are attached to the two orientable fingers. The purpose of the orientation transmission is to use one actuator to drive the two rotating fingers. This rotation is synchronized by the gearing system and the fingers rotate in opposite directions. The input gear, attached to the input shaft, directly drives the finger 1 gear. The second finger gear, driven via a free gear, is attached to a free shaft to obtain a rotation of the second finger in a direction opposite from that of the first finger.

3. ACTUATION SYSTEM

In order to operate the gripper smoothly and flexibly, we need to integrate electronic part and controller into the gripper mechanical design.

3.1. Main controller part

In this project, we used board Arduino Mega 2560 - a type of Single-board microcontroller. Because of its high efficiency, easy to work with and is commonly used in many 3D printers.
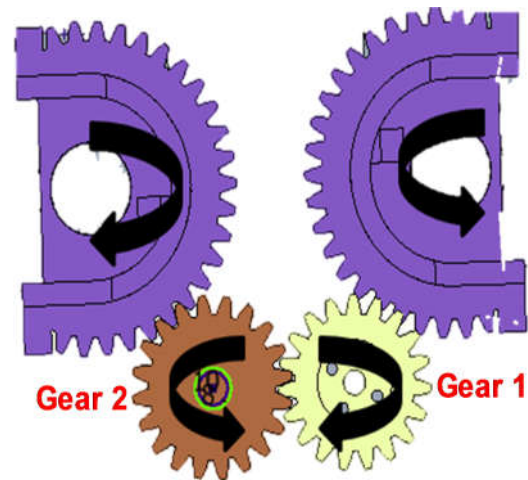
Figure 10. The orientation mechanism
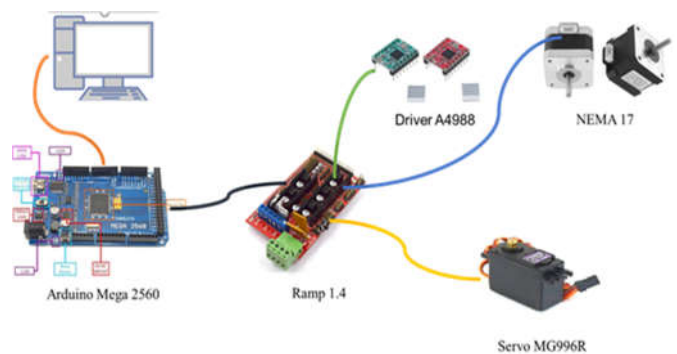
Figure 11. The whole diagram of control system
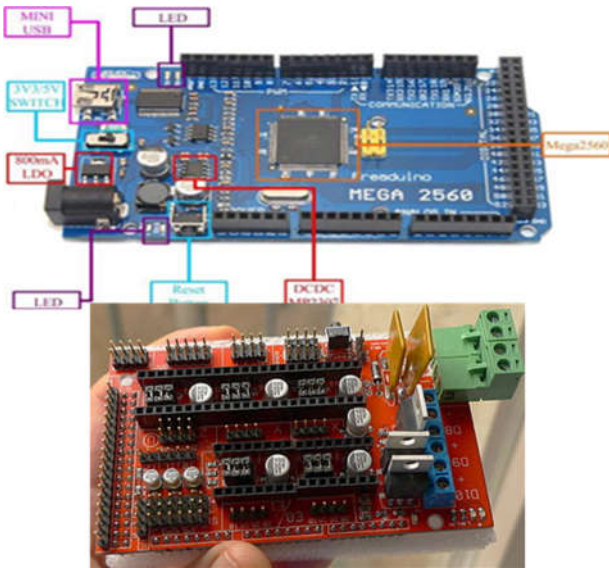
Figure 12. Arduino Mega 2560 and RAMPS 1.4 circuit

Along with board Arduino Mega 2560, we used RAMPS 1.4 motherboard. RAMPS 1.4 is a board that serves as the interface between the Arduino Mega - the controller computer - and the electronic devices in the gripper. The board is accessible, reliable, easy to replaced.

3.2. Stepper driver and engines

A stepper drive is the driver circuit that controls how the stepper motor operates. The two most commonly used driver is driver A4988 and DRV8825. We used A4988 in this project. Stepper drives work by sending current through various phases in pulses to the stepper motor. The driver carries out two primary functions: sequencing the phases and controlling the phase current.

Figure 13. A4988 stepper driver and engines

4. SIMULATION AND EXPERIMENTAL RESULTS

4.1. Modeling and simulation results

We modify the gear model from the couple two spinning inertias with a simple gear from Simulink example to modeling the first stage and the compound planetary gear model for the second stage. We conduct this simulation to observe the output torque of the annulus, carrier, and sun.
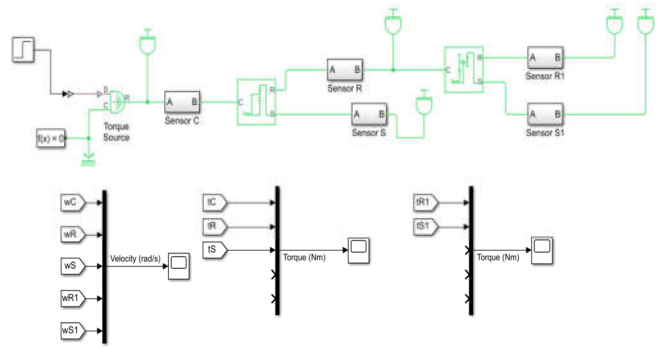
Figure 14. Planetary Gear Differential Simulink block
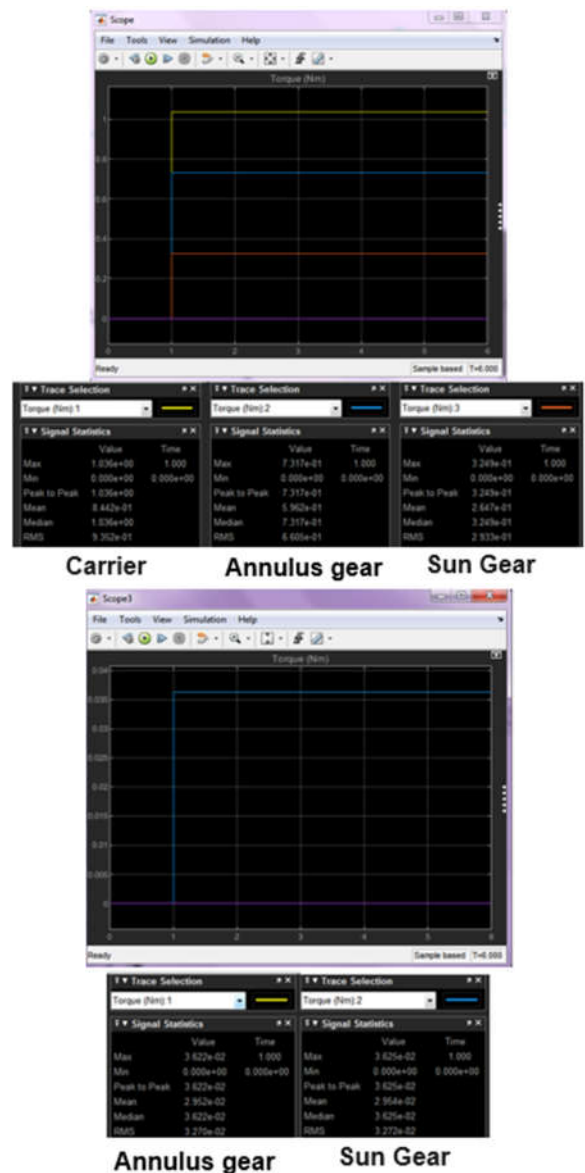
Figure 15. First stage and second stage simulation results

This gripper can perform power grasp, which means that the fingers envelope the object and pinch grasp, which mean that the distal phalanges maintain parallel to each other with objects. Both configuration is shown in Fig. 15.
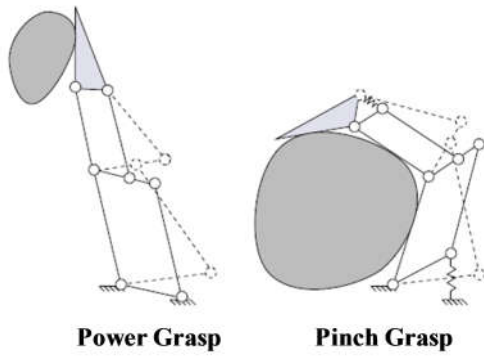
Figure 16. Object grasp [3]
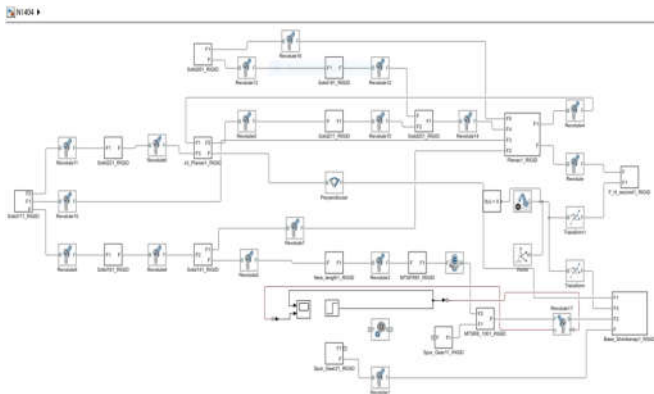
Figure 17. Simscape Multibody model of the whole system

This mechanism in Fig.16 is composed of two parallelograms mounted in series. It is coupled to the phalanges of the finger but not to the other links of the shape adaptation mechanism (it is moving on a parallel yet distinct plane). Its aim is to constrain the orientation of the distal phalanx relatively to the palm until contact is made with the object, without sensors to detect this contact. If the latter happens with the distal phalanx itself, the finger is fixed (assuming that the object is seized). On the other hand, if contact is made with the proximal or intermediate phalanx, the mechanism is automatically disengaged and the distal phalanx can close on the object.

(a)

(b)
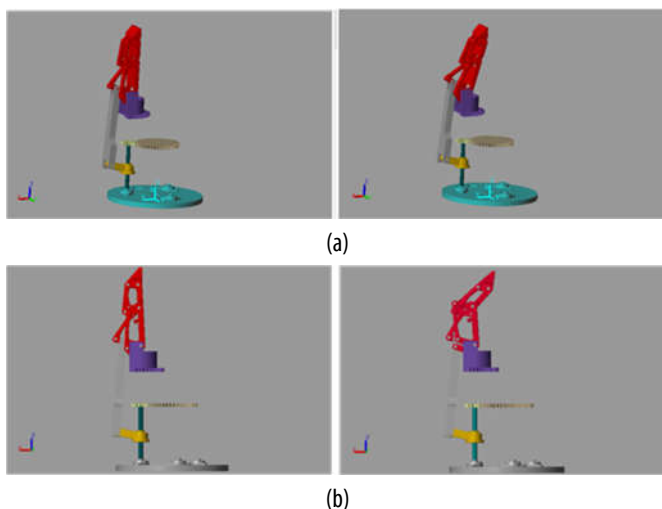
Figure 18. Pinch grasp (a) and power grasp (b) simulation results

4.2. Experimental results

We conducted experiments to test the grasping and capabilities of the three-fingered gripper. Fig.19 shows the objects used in the experiments. We fashioned a 85mm in diameter bell pepper, a 73mm in diameter tomato, a 55mm in diameter tomato and a cylinder.

Figure 19. Graspable objects for the experiments

In cylindrical test, two fingers point in the same direction while the third one points in the opposite direction and moves between the other two. This is preferred configuration to grasp cylindrical/prismatic objects or objects where one dimension is significantly larger than those of the hand Fig. 20.

Figure 20. Test with cylindrical object

In the spherical test, the three fingers are oriented towards the centroid of the triangle formed by the base joints of the fingers. This configuration is the preferred choice to perform enveloping grasps of objects with sizes close to the size of the hand or with no distinct particular axis.

Figure 21. Test with spherical object

In the planar configuration, two fingers are directly facing each other and the third finger is not used. This configuration is used for pinch grasps, usually of objects with small dimensions.

a) 55 mm tomato   b) 73 mm tomato   c) 85 mm bell pepper
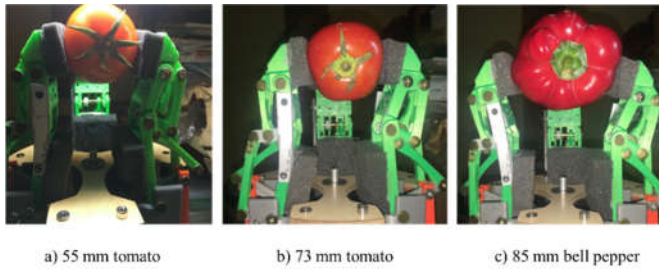
Figure 22. Planar configuration test

5. CONCLUSIONS

This paper presented under-actuated 3-finger gripper design with one actuator which can perform a wide range of grasping tasks. We had grasped the - overview of the robot's gripper theory, concepts, mechanisms, operating principles and more specifically about the under-actuated robot gripper. The simplicity of the gripper elements and mechanisms allow their manufacturing with 3D printing technology and additional off-the-shelf components. The operation of the prototype is evaluated by using numerical simulation in Matlab/Simulink and several experimental tests. From the experimental results, it was confirmed that our proposed gripper could grasp variously shaped objects.

However, further work is required. The gripper is still cumbersome because the parts are made from the rapid prototyping method. And the controller built for this gripper is still very basic. So, in future work, we will add the tactile sensor at each finger and develop a control algorithm to control the clamping force of this mechanism in order to improve grasp performance. The gripper will be mounted to an industrial robot for evaluating grasping ability in real-life scenarios.

REFERENCES

[1]. A. Kakogawa, et al., 2016. *Underactuated modular finger with pull-in mechanism for a robotic gripper*. ROBIO, pp. 556-561.

[2]. V.B. Bhandari, 2010. *Design of Machine Elements*. Tata McGraw-Hill Education.

[3]. Birglen L., Lalibert´e T., Gosselin C., 2008. *Underactuated Robotic Hands*. Springer-Verlag, ISBN 978-3-540-77458-7.

[4]. Hartenberg R. S., Denavit J., 1964. *Kinematic synthesis of Linkages*. S. M.Drake, Robert, JR, J.Kline, Ed.

[5]. Matei Ciocarlie, Fernando Mier Hicks, Scott Stanford, 2013. *Kinetic and Dimensional Optimization for a Tendon-driven Gripper*. In International Conference on Robotics and Automation, pages 2736 -2743.

[6]. RR Ma, LU Odhner, AM Dollar, 2013. *A modular, open-source 3d printed underactuated hand*. In IEEE International Conference on Robotics and Automation (ICRA), pages 2722-2728, Karlsruhe, Germany.

[7]. Pierluigi Rea, 2011. *On the Design of Underactuated Finger Mechanisms for Robotic Hands, Advances in Mechatronics*. Horacio Martinez-Alfaro, Intech Open.

[8]. J. Schuurmans, R.Q. van der Linde, D.H. Plettenburg, F.C. van der Helm, 2007. *Grasp force optimization in the design of an underactuated robotic hand*. IEEE 10th International Conference on Rehabilitation Robotics.

[9]. Telegenov Kuat, Tlegenov Yedige, Hussain Shahid, Shintemirov Almas, 2015. *Preliminary Design and Analysis of a Three Finger Underactuated Adaptive End Effector with a Breakaway Clutch Mechanism*. Journal of Robotics and Mechatronics Vol. 27, No. 5.

[10]. V. Vullo, 2020. *Gear Trains and Planetary Gears*. In: Gears. Springer Series in Solid and Structural Mechanics, vol 10. Springer, pages 695-770.

[11]. Zhang Yuru, Han Z., Zhang H., Shang X., Wang T., Guo Weidong, Gruver William, 2001. *Design and control of the BUAA four-fingered hand*. Proceedings - IEEE International Conference on Robotics and Automation. 3. 2517 - 2522 vol.3. 10.1109/ROBOT.2001.933001.

THÔNG TIN TÁC GIẢ

Lê Hoài Nam, Trần Cường Hưng, Nguyễn Ngọc Linh

Trường Đại học Công nghệ, Đại học Quốc gia Hà Nội